

Redundancy in the information transmission in a two-step cascade

Ayan Biswas* and Suman K Banik†

Department of Chemistry, Bose Institute, 93/1 A P C Road, Kolkata 700009, India

(Dated: 18 April, 2016)

We present a stochastic framework to study signal transmission in a generic two-step cascade $S \rightarrow X \rightarrow Y$. Starting from a set of Langevin equations obeying Gaussian noise processes we calculate the variance and covariance while considering both linear and nonlinear production terms for different biochemical species of the cascade. These quantities are then used to calculate the net synergy within the purview of partial information decomposition. We show that redundancy in information transmission is essentially an important consequence of Markovian property of the two-step cascade motif. We also show that redundancy increases fidelity of the signalling pathway.

PACS numbers: 87.10.-e, 05.40.-a, 87.18.Tt, 87.18.Vf

I. INTRODUCTION

A living system sustains in the diverse and continuously changing environment. In order to respond to the changes made in the surroundings, every living species developed complex signal transmission networks over the evolutionary time scale [1, 2]. The main purpose of these networks is to transmit the extracellular changes reliably and efficiently to the cell. In addition, these networks take care of different biochemical changes that are taking place within the cell. A typical signalling cascade comprises of one or several components of biochemical origin. The interactions between these components are probabilistic in nature, thus giving rise to stochastic kinetics. One of the tools to figure out the signal transmission mechanism in a fluctuating environment is information theory [3, 4]. The formalism of information theory provides a quantification of information transfer between the source (signal) and the target (response). The measure of information transmission is characterized by mutual information (MI), that quantifies the common information content of the source and the target. Moreover, information theory provides a measure of fidelity of the signalling pathway [5–15].

The notion of MI is conceptualized as the intersection of the entropy spaces of two stochastic variables [3, 4]. Hence, MI signifies the average reduction in the uncertainty of prediction of one random variable when knowledge of another random variable is available. However, this information theoretic measure is symmetric in its argument random variables signifying the ‘mutual’ attribution linked to it. For a generic two-step cascade (TSC) $S \rightarrow X \rightarrow Y$, although, MI among three variables is an ill defined concept, its usage can be validated if one considers $I(s; x, y)$ to be the MI that the source variable S shares with the pair of target variables X and Y . It is thus interesting to investigate whether the three variable MI can be utilised in such a way to shed light

on various types of informational relationship among the three stochastic variables (S , X , and Y). One prevalent approach in this respect is known as partial information decomposition (PID) [16, 17]. Following the formalism of PID one can define an information theoretic measure, the net synergy $\Delta I(s; x, y)$, in terms of two and three variable MI-s [16–20]

$$\Delta I(s; x, y) = I(s; x, y) - I(s; x) - I(s; y). \quad (1)$$

At this point, one should take note of the fact that the net synergy can be both positive ($\Delta I > 0$) and negative ($\Delta I < 0$) valued. Information theoretically, positive net synergy implies synergistic aspect of the target variables is prevalent over the extent of redundant character. Negative net synergy conveys precisely the opposite implication. Positive net synergy indicates the information shared between the source S and the targets (X , Y) taken together as a single target is more than the sum of the information shared between S and the targets X , Y considered individually in turn. Negative net synergy indicates separately the targets share more information with the source than while considered together as a single target. Zero net synergy ($\Delta I = 0$) is an interesting case to mention as it means that the targets X and Y are informationally independent of each other since the information shared between the source and the targets does not depend on whether one takes the targets individually or together as a single target to compute different mutual information terms. As per the definition of the net synergy stated in Eq. (1), it is maximum while the total information is synergistic and assumes a minimum value when the total information is purely redundant in nature. In this study, we do not quantify the separate identification of synergy and redundancy. Rather, we conceive the quantity of interest here as redundant synergy. Information theoretically, the net synergy serves as a quantification marker of information independence between the random variables often characterized as source and target variables [18]. Although, the tags of source(s) and target(s) are not strict enough in information theoretic sense but while dealing with cascades or directed networks, in general, such classifications can be done suitably as the phenomenology or experimental realities demand.

* ayanbiswas@jcbose.ac.in

† Corresponding author: skbanik@jcbose.ac.in

To understand the redundancy in the information transmission in biochemical processes we undertake the kinetics associated with a generic TSC Motif $S \rightarrow X \rightarrow Y$. The dynamics related to the TSC motif could be linear or nonlinear in nature and provides analytical solution at steady state within the purview of Gaussian noise processes. In this connection, it is important to mention theoretical analysis performed on different biochemical motifs obeying Gaussian noise processes [7, 8, 13, 20–27]. In this set of works, the theoretical analysis was performed using linear noise approximation [28–30] that provides exact expressions upto second moments. Recent theoretical development [27] shows that linear noise approximation is not only limited for high copy number conditions but can also be exact up to second moments for some systems with second-order reactions. In this case, it is found that the fluctuations associated with at least one of the species participating in each of the second-order reaction are Poissonian and uncorrelated with the fluctuations of the other species.

II. THE MODEL

The set of Langevin equations governing the dynamics of a TSC motif can be written as,

$$\frac{ds}{dt} = f_s(s) - \mu_s s + \xi_s(t), \quad (2)$$

$$\frac{dx}{dt} = f_x(s, x) - \mu_x x + \xi_x(t), \quad (3)$$

$$\frac{dy}{dt} = f_y(s, x, y) - \mu_y y + \xi_y(t), \quad (4)$$

where s , x and y are three nodes of the cascade representing three different gene products. Here f_i -s and μ_i -s ($i = s, x, y$) are the synthesis and degradation rates of the components S, X and Y, respectively. Depending on the nature of interaction, the synthesis terms could be linear or nonlinear in nature. The noise terms $\xi_i(t)$ are independent and Gaussian-distributed with properties $\langle \xi_i(t) \rangle = 0$ and $\langle \xi_i(t) \xi_j(t') \rangle = \langle |\xi_i|^2 \rangle \delta_{ij} \delta(t - t')$, where $\langle |\xi_i|^2 \rangle = \langle f_i \rangle + \mu_i \langle i \rangle = 2\mu_i \langle i \rangle$ for $i = s, x, y$ [22–24, 28, 29, 31–33]. The quantities $\langle i \rangle = \langle s \rangle, \langle x \rangle, \langle y \rangle$ are the steady state (coarse-grained) values of the respective species [34]. We now expand Eqs. (2-4) around steady state $\delta z(t) = z(t) - \langle z \rangle$, where $\langle z \rangle$ is the average population of z at steady state and obtain,

$$\frac{d\delta \mathbf{A}}{dt} = \mathbf{J}_{A=\langle A \rangle} \delta \mathbf{A}(t) + \mathbf{\Theta}(t). \quad (5)$$

Here $\delta \mathbf{A}$ and $\mathbf{\Theta}$ are the fluctuations matrix and the noise matrix, respectively, with

$$\delta \mathbf{A} = \begin{pmatrix} \delta s \\ \delta x \\ \delta y \end{pmatrix} \text{ and } \mathbf{\Theta} = \begin{pmatrix} \xi_s \\ \xi_x \\ \xi_y \end{pmatrix}.$$

\mathbf{J} is the Jacobian matrix evaluated at steady state

$$\mathbf{J} = \begin{pmatrix} f'_{s,s}(\langle s \rangle) - \mu_s & 0 & 0 \\ f'_{x,s}(\langle s \rangle, \langle x \rangle) & f'_{x,x}(\langle s \rangle, \langle x \rangle) - \mu_x & 0 \\ f'_{y,s}(\langle s \rangle, \langle x \rangle, \langle y \rangle) & f'_{y,x}(\langle s \rangle, \langle x \rangle, \langle y \rangle) & f'_{y,y}(\langle s \rangle, \langle x \rangle, \langle y \rangle) - \mu_y \end{pmatrix}$$

where $f'_{s,s}(\langle s \rangle)$ implies f_s has been differentiated with respect to s and is evaluated at $s = \langle s \rangle$, and so on. To calculate the variance and covariance of different species of the TSC motif, we use the Lyapunov equation at steady state [28, 29, 32, 35, 36]

$$\mathbf{J}\mathbf{\Sigma} + \mathbf{\Sigma}\mathbf{J}^T + \mathbf{D} = 0. \quad (6)$$

Here, $\mathbf{\Sigma}$ is the covariance matrix and $\mathbf{D} = \langle \mathbf{\Theta}\mathbf{\Theta}^T \rangle$ is the diffusion matrix due to different noise strengths. The notation $\langle \dots \rangle$ stands for ensemble average and T is the transpose of a matrix. For linear interaction [7, 13, 22, 34, 37, 38]

$$f_s = k_s, f_x = k_x s \text{ and } f_y = k_y x,$$

solution of Eq. (6) provides analytical expressions of variance and covariance associated with s , x and y

$$\Sigma(s) = \langle s \rangle, \Sigma(s, x) = \frac{k_x \langle s \rangle}{\mu_s + \mu_x},$$

$$\Sigma(s, y) = \frac{k_y k_x \langle s \rangle}{(\mu_s + \mu_x)(\mu_s + \mu_y)},$$

$$\Sigma(x) = \langle x \rangle + \frac{k_x^2 \langle s \rangle}{\mu_x(\mu_s + \mu_x)},$$

$$\Sigma(x, y) = \frac{k_y}{\mu_x + \mu_y} \Sigma(x) + \frac{k_x}{\mu_x + \mu_y} \Sigma(s, y),$$

$$\Sigma(y) = \langle y \rangle + \frac{k_y}{\mu_y} \Sigma(x, y).$$

Similarly, for nonlinear interaction [39–42]

$$f_s = k_s, f_x = k_x \frac{s^n}{K_1^n + s^n} \text{ and } f_y = k_y \frac{x^n}{K_2^n + x^n},$$

we have from Eq. (6)

$$\Sigma(s) = \langle s \rangle, \Sigma(s, x) = \frac{nk_x K_1^n \langle s \rangle^n}{(K_1^n + \langle s \rangle^n)^2 (\mu_s + \mu_x)},$$

$$\Sigma(s, y) = \frac{nk_y K_2^n \langle x \rangle^{n-1} \Sigma(s, x)}{(K_2^n + \langle x \rangle^n)^2 (\mu_s + \mu_y)},$$

$$\Sigma(x) = \langle x \rangle + \frac{nk_x K_1^n \langle s \rangle^{n-1} \Sigma(s, x)}{(K_1^n + \langle s \rangle^n)^2 \mu_x},$$

$$\Sigma(x, y) = \frac{nk_y K_2^n \langle x \rangle^{n-1} \Sigma(x)}{(K_2^n + \langle x \rangle^n)^2 (\mu_x + \mu_y)} + \frac{nk_x K_1^n \langle s \rangle^{n-1} \Sigma(s, y)}{(K_1^n + \langle s \rangle^n)^2 (\mu_x + \mu_y)},$$

$$\Sigma(y) = \langle y \rangle + \frac{nk_y K_2^n \langle x \rangle^{n-1} \Sigma(x, y)}{(K_2^n + \langle x \rangle^n)^2 \mu_y}.$$

We now quantify the MI-s associated with the signalling cascade $S \rightarrow X \rightarrow Y$. For s , x and y assumed

to be Gaussian random variables one can express the net synergy associated with TSC motif as follows [17]

$$\Delta I(s; x, y) = \frac{1}{2} \left[\log_2 \left(\frac{\det \Sigma(s)}{\det \Sigma(s|x, y)} \right) - \log_2 \left(\frac{\det \Sigma(s)}{\det \Sigma(s|x)} \right) - \log_2 \left(\frac{\det \Sigma(s)}{\det \Sigma(s|y)} \right) \right]. \quad (7)$$

The usage of base 2 in the logarithm functions suggests that the net synergy is calculated in the units of ‘bits’. The first, second and the third term on the right hand side of Eq. (7) corresponds to $I(s; x, y)$, $I(s; x)$ and $I(s; y)$, respectively. The definitions of various conditional variances used in Eq. (7) are

$$\Sigma(s|x) =: \Sigma(s) - \Sigma(s, x)(\Sigma(x))^{-1}\Sigma(x, s), \quad (8)$$

$$\Sigma(s|y) =: \Sigma(s) - \Sigma(s, y)(\Sigma(y))^{-1}\Sigma(y, s), \quad (9)$$

$$\Sigma(s|x, y) =: \Sigma(s) - \begin{pmatrix} \Sigma(s, x) & \Sigma(s, y) \end{pmatrix} \begin{pmatrix} \Sigma(x) & \Sigma(x, y) \\ \Sigma(y, x) & \Sigma(y, y) \end{pmatrix}^{-1} \begin{pmatrix} \Sigma(x, s) \\ \Sigma(y, s) \end{pmatrix}. \quad (10)$$

The expression of $\Sigma(s|x, y)$ after completing the matrix multiplication yields

$$\begin{aligned} \Sigma(s|x, y) = & \Sigma(s) - (1/\mathcal{D})[\Sigma(y)\Sigma^2(s, x) \\ & - 2\Sigma(s, x)\Sigma(s, y)\Sigma(x, y) \\ & + \Sigma(x)\Sigma^2(s, y)], \end{aligned} \quad (11)$$

with $\mathcal{D} =: \Sigma(x)\Sigma(y) - \Sigma^2(x, y)$.

III. RESULTS AND DISCUSSION

While calculating the net synergy $\Delta I(s; x, y)$, various mutual information ($I(s; x, y)$, $I(s; x)$ and $I(s; y)$) and signal-to-noise ratio (SNR) we use $\langle s \rangle = 10$, $\langle x \rangle = 100$ and $\langle y \rangle = 100$ for both linear and nonlinear interactions. This helps to compare the behaviour of the motif at steady state for different interactions as the level of system components at steady state performs the optimal function [1]. To check the validity of our theoretical expressions we also carry out numerical simulation following stochastic simulation algorithm [43, 44] while considering the kinetics associated with the linear and nonlinear interactions.

In Fig. 1, we show the profiles of the net synergy $\Delta I(s; x, y)$, various mutual information ($I(s; x, y)$, $I(s; x)$ and $I(s; y)$) and SNR as functions of input relaxation rate constant μ_s for both linear and nonlinear interactions ($n = 1$). The lines are due to theoretical calculation and the symbols are generated from stochastic simulation [43, 44]. In Fig. 1(a) and 1(d), both the net synergy profiles grow hyperbolically as μ_s is increased and move towards $\Delta I = 0$. For low value of μ_s the domain of redundancy decreases as the interaction between different

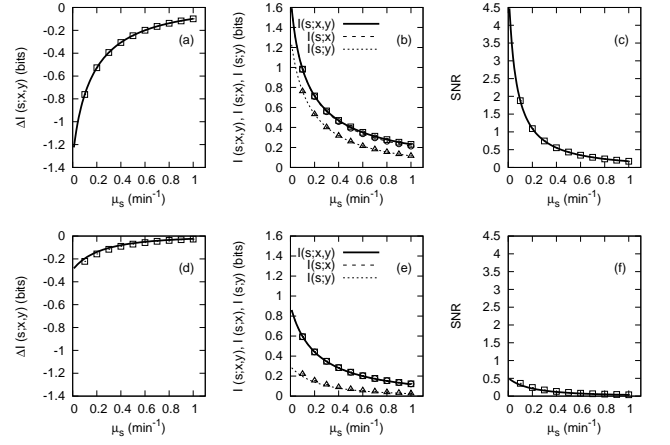


FIG. 1. The net synergy [(a), (d)], mutual information [(b), (e)] and SNR [(c), (f)] profiles as functions of μ_s . (a)-(c) are for linear interaction and (d)-(f) are for nonlinear interaction. The lines are theoretical results and the symbols are generated from stochastic simulation. The simulation results are average of 10^5 trajectories. The parameters common to both linear and nonlinear interactions are $\langle s \rangle = 10$, $\langle x \rangle = 100$, $\langle y \rangle = 100$, $\mu_x = 0.5 \text{ min}^{-1}$, $\mu_y = 5 \text{ min}^{-1}$ and $k_s = 10\mu_s$. For linear interaction $k_x = 10\mu_x$ and $k_y = \mu_y$. For nonlinear interaction $k_x = \mu_x \langle x \rangle (K_1 + \langle s \rangle) / \langle s \rangle$, $k_y = \mu_y \langle y \rangle (K_2 + \langle x \rangle) / \langle x \rangle$, $K_1 = 10$, $K_2 = 100$ and $n = 1$.

system components changes from linear (see Fig. 1(a)) to nonlinear (see Fig. 1(d)). In case of nonlinear interaction with $n = 1$, fluctuations associated with the production of X decrease as $f'_{x,s}(\text{linear}) > f'_{x,s}(\text{nonlinear})$ for fixed copy number and parameter set. Similar relation holds good for Y also, i.e., $f'_{y,x}(\text{linear}) > f'_{y,x}(\text{nonlinear})$. These effects together lower the magnitudes of variance and covariance associated with X and Y thus lowering the magnitudes of different MI-s. As a result, the domain of redundancy decreases.

As mentioned earlier, we are only interested in the difference between synergy and redundancy since their individual values can not be determined within the purview of PID adopted in the present work. If at all one tries to infer synergy from the net synergy, one may consider the net synergy as redundant synergy of some kind [16]. To understand the nature of the net synergy we look at the profiles of its three ingredients, viz., $I(s; x, y)$, $I(s; x)$ and $I(s; y)$ as functions of μ_s . In Fig. 1(b) and 1(e), $I(s; x, y)$ and $I(s; x)$ are nearly equal while $I(s; y)$ assumes a lower value compared to the other two expressions of MI. This result suggests that in the TSC motif the relevant information is lost and is never regained while getting transduced from the source to the output. This loss cannot be undone or compensated by any kind of manipulation in the signal transduction pathway. From the information theoretic point of view, this is a consequence of data processing inequality (DPI) [4]. Within the framework of Markov chain property we have $I(s; x, y) = I(s; x)$

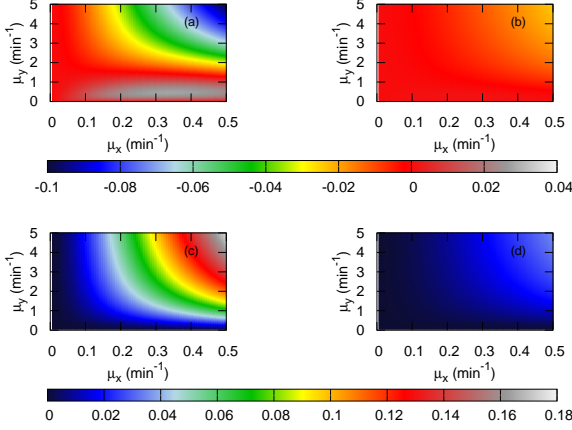


FIG. 2. (color online) Two-dimensional maps of the net synergy (in bits) [(a), (b)] and SNR [(c), (d)] as functions of μ_x and μ_y for $\mu_s = 1 \text{ min}^{-1}$. (a), (c) are for linear interaction and (b), (d) are for nonlinear interaction with $n = 1$. The parameters are same as in Fig. 1 except $\mu_s = 1 \text{ min}^{-1}$. The maps are generated using theoretical expressions.

and $I(s; x) \geq I(s; y)$ where the inequality expression is due to DPI. From Fig. 1(b) and 1(e) it is clear that $I(s; x, y) \approx I(s; x)$ and $I(s; x) > I(s; y)$. Recalling the expression of the net synergy, we notice that the first two terms ($I(s; x, y)$ and $I(s; x)$) nearly cancel each other and we are left with $\Delta I(s; x, y) \approx -I(s; y)$ that generates the net synergy profiles shown in Fig. 1. Introduction of non-linearity reduces the contribution of $I(s; y)$ (the dotted line with triangles in Fig. 1(e)) in the expression of the net synergy. Whereas, for linear interaction the same has a relatively high contribution (the dotted line with triangles in Fig. 1(b)). This in turn supports our argument of lowering of redundancy due to lesser contribution of $I(s; y)$ for nonlinear interaction.

The net synergy profiles and the contributions of individual MI-s suggest that with an increase of μ_s the common or redundant information between X and Y decreases. A consequence of redundancy gets reflected through SNR defined as $\Sigma^2(s, y)/(\Sigma(s)\Sigma(y) - \Sigma^2(s, y))$. The profiles of SNR are shown in Fig. 1(c) and 1(f). To keep stock of the SNR profiles, one should remember that information flow and noise propagation are by default antagonistic to each other. As redundant information increases, there are lesser chances that the system would lose any valuable information since even if some amount of information gets corrupted by noise along the signalling pathway, there are possible replacements of lost information due to its redundancy property. In this way,

redundancy empowers fidelity (or SNR) of the signalling pathway. The SNR profiles shown in Fig. 1(c) and 1(f) thus show opposite trend as compared to that of the net synergy.

From the nature of the net synergy profiles shown in Fig. 1, one is left with the impression that the net synergy is constrained only in the negative domain. To explore further we scan the full parameter range of μ_x and μ_y for $\mu_s = 1 \text{ min}^{-1}$. The resultant two-dimensional map of the net synergy and SNR are shown in Fig. 2. Fig. 2(a) suggests that for linear interaction a region exists with $\Delta I > 0$. Similar trend is observed for nonlinear interaction in Fig. 2(b). Since the values of individual MI-s are always ≥ 0 [4], the positive value of the net synergy suggests that $I(s; x, y) > I(s; x) + I(s; y)$ (see the expression of the net synergy given in Eq. (1)). As expected, opposite trend is observed in SNR (Fig. 2(c) and 2(d)). For $\Delta I > 0$ and $\Delta I < 0$ we have low and high SNR, respectively.

IV. CONCLUSION

To summarize, we have investigated how different constituents of a generic TSC motif are related to each other in information theoretic sense. To investigate such mutual dependencies, we explored the concept of net synergy, an essential information theoretic measure due to the formalism of partial information decomposition. The two variable and three variable mutual information quantities have been computed in terms of variance and covariance of the Gaussian random variables representing the components of the TSC motif. In this study, we have tuned the signal by changing the degradation rate of the source (μ_s) and have quantified the three MI-s, the net synergy and the SNR for linear and nonlinear interactions. Our results show that $I(s; x, y)$ and $I(s; x)$ are nearly equal. As a consequence of Markov chain property, the net synergy $\Delta I(s; x, y)$ picks up contribution mostly from $I(s; y)$, thus showing redundancy. Based on our findings, we argue that redundancy can increase the fidelity of the TSC motif as redundant information enhances SNR in the system. We further make a thorough scan of the parameter space and notice a region of synergy where $I(s; x, y) > I(s; x) + I(s; y)$.

ACKNOWLEDGMENTS

We thank Alok Kumar Maity for fruitful discussion. Financial support from Institutional Programme VI - Development of Systems Biology, Bose Institute, Kolkata is thankfully acknowledged.

[1] U. Alon, *An Introduction to Systems Biology: Design Principles of Biological Circuits* (CRC Press, Boca Ra-

ton, 2006).

- [2] U. Alon, Nat. Rev. Genet. **8**, 450 (2007).
- [3] C. E. Shannon, Bell. Syst. Tech. J **27**, 379 (1948).
- [4] T. M. Cover and J. A. Thomas, *Elements of Information Theory* (Wiley-Interscience, New York, 1991).
- [5] A. Borst and F. E. Theunissen, Nat. Neurosci. **2**, 947 (1999).
- [6] P. P. Mitra and J. B. Stark, Nature **411**, 1027 (2001).
- [7] E. Ziv, I. Nemenman, and C. H. Wiggins, PLoS ONE **2**, e1077 (2007).
- [8] F. Tostevin and P. R. ten Wolde, Phys. Rev. E **81**, 061917 (2010).
- [9] I. Lestas, G. Vinnicombe, and J. Paulsson, Nature **467**, 174 (2010).
- [10] R. Cheong, A. Rhee, C. J. Wang, I. Nemenman, and A. Levchenko, Science **334**, 354 (2011).
- [11] G. Tkačik and A. M. Walczak, J. Phys. Condens. Matter **23**, 153102 (2011).
- [12] C. G. Bowsher, M. Voliotis, and P. S. Swain, PLoS Comput. Biol. **9**, e1002965 (2013).
- [13] A. K. Maity, P. Chaudhury, and S. K. Banik, PLoS ONE **10**, e0123242 (2015).
- [14] S. S. Mc Mahon, A. Sim, S. Filippi, R. Johnson, J. Liepe, D. Smith, and M. P. Stumpf, Semin. Cell Dev. Biol. **35**, 98 (2014).
- [15] L. S. Tsimring, Rep. Prog. Phys. **77**, 026601 (2014).
- [16] P. L. Williams and R. D. Beer (2010), arXiv: cs.IT/1004.2515.
- [17] A. B. Barrett, Phys. Rev. E **91**, 052802 (2015).
- [18] E. Schneidman, W. Bialek, and M. J. Berry, J. Neurosci. **23**, 11539 (2003).
- [19] A. S. Hansen and E. K. O'Shea, Elife **4**, e06559 (2015).
- [20] A. K. Maity, P. Chaudhury, and S. K. Banik (2015), arXiv: q-bio.MN/1510.04799.
- [21] W. Bialek and S. Setayeshgar, Proc. Natl. Acad. Sci. U.S.A. **102**, 10040 (2005).
- [22] W. H. de Ronde, F. Tostevin, and P. R. ten Wolde, Phys. Rev. E **82**, 031914 (2010).
- [23] S. Tănase-Nicola, P. B. Warren, and P. R. ten Wolde, Phys. Rev. Lett. **97**, 068102 (2006).
- [24] P. B. Warren, S. Tănase-Nicola, and P. R. ten Wolde, J. Chem. Phys. **125**, 144904 (2006).
- [25] F. J. Bruggeman, N. Blüthgen, and H. V. Westerhoff, PLoS Comput. Biol. **5**, e1000506 (2009).
- [26] A. K. Maity, A. Bandyopadhyay, P. Chaudhury, and S. K. Banik, Phys. Rev. E **89**, 032713 (2014).
- [27] R. Grima, Phys. Rev. E **92**, 042124 (2015).
- [28] N. G. van Kampen, *Stochastic Processes in Physics and Chemistry*, 3rd ed. (North-Holland, Amsterdam, 2007).
- [29] J. Elf and M. Ehrenberg, Genome Res. **13**, 2475 (2003).
- [30] D. T. Gillespie, J. Chem. Phys. **113**, 297 (2000).
- [31] P. S. Swain, J. Mol. Biol. **344**, 965 (2004).
- [32] J. Paulsson, Nature **427**, 415 (2004).
- [33] P. Mehta, S. Goyal, and N. S. Wingreen, Mol. Syst. Biol. **4**, 221 (2008).
- [34] W. H. de Ronde, F. Tostevin, and P. R. ten Wolde, Phys. Rev. E **86**, 021913 (2012).
- [35] J. Keizer, *Statistical Thermodynamics of Nonequilibrium Processes* (Springer-Verlag, Berlin, 1987).
- [36] J. Paulsson, Phys Life Rev **2**, 157 (2005).
- [37] G. Tkačik, C. G. Callan, and W. Bialek, Proc. Natl. Acad. Sci. U.S.A. **105**, 12265 (2008).
- [38] G. Tkačik, A. M. Walczak, and W. Bialek, Phys. Rev. E **80**, 031920 (2009).
- [39] L. Bintu, N. E. Buchler, H. G. Garcia, U. Gerland, T. Hwa, J. Kondev, and R. Phillips, Curr. Opin. Genet. Dev. **15**, 116 (2005).
- [40] W. Bialek and S. Setayeshgar, Phys. Rev. Lett. **100**, 258101 (2008).
- [41] G. Tkačik, C. G. Callan, and W. Bialek, Phys. Rev. E **78**, 011910 (2008).
- [42] G. Tkačik, T. Gregor, and W. Bialek, PLoS ONE **3**, e2774 (2008).
- [43] D. T. Gillespie, J. Comp. Phys. **22**, 403 (1976).
- [44] D. T. Gillespie, J. Phys. Chem. **81**, 2340 (1977).